Composite Structures 187 (2018) 27–35

Contents lists available at ScienceDirect

Composite Structures

journal homepage: www.elsevier.com/locate/compstruct

Investigation on the static and dynamic behaviors of non-pneumatic tires with honeycomb spokes

Xiaochao Jin[a], Cheng Hou[a], Xueling Fan[a,*], Yongle Sun[b], Jinan Lv[c], Chunsheng Lu[d]

[a] State Key Laboratory for Strength and Vibration of Mechanical Structures, School of Aerospace Engineering, Xi'an Jiaotong University, Xi'an 710049, China
[b] School of Mechanical, Aerospace and Civil Engineering, The University of Manchester, Sackville Street, Manchester M13 9PL, UK
[c] China Academy of Aerospace Aerodynamics (CAAA), Beijing 100074, China
[d] School of Civil and Mechanical Engineering, Curtin University, Perth, WA 6845, Australia

ARTICLE INFO

Keywords:
Non-pneumatic tire
Honeycomb spokes
Contact pressure
Rolling resistance

ABSTRACT

Non-pneumatic tires (NPTs) have wide application prospects due to their advantages of no run-flat, no need of air pressure maintenance, and low rolling resistance. In this paper, the static and dynamic behaviors of NPTs with different honeycomb spokes were investigated. Based on the static behavior of three types of NPTs with the same cell wall thickness of honeycomb or the same reference load carrying capacity, it is shown that the maximum stresses in spokes and tread of a NPT are much lower than that of traditional pneumatic tires, but its load carrying capacity is higher than the latter. In comparison with the dynamic behavior of three types of NPTs designed with the same load carrying capacity, it is found that the stress level in spokes and tread under dynamic loading are higher than that under static loading. The rolling resistance of NPTs with the smallest cell expanding angle is lowest, which is due to the lowest mass and smallest deformation of honeycomb spokes. Taking all these factors into account, it is suggested that an optimal NPT in applications is one with a small cell expanding angle and wall thickness.

1. Introduction

Since non-pneumatic tires (NPTs) were proposed, they have received increasing attention owing to their remarkable advantages such as no run-flat, no need of air pressure maintenance, and low rolling resistance, compared with traditional pneumatic tires [1,2]. A typical NPT usually consists of a hub, a number of flexible spokes, a shear ring and a tread. Normally, tread is made of synthetic rubber, and shear ring is a composite structure composed of a shear band with two circumferential reinforcements (i.e., inner and outer rings). Flexible spokes are the most unique components in NPTs and they are based on polyurethane materials. Uniform and flexible spokes that are designed to connect the composite shear ring and hub of NPTs are mainly deformed by compression, tension, bending or buckling during rolling.

The spokes of a NPT require a combination of stiffness and resilience under cyclic tension-compression loading, which brings a challenge to the selection of materials and structural design. Cellular materials and their constructed structures can be applied to meet these requirements, and honeycomb spokes have a great potential in NPTs. Honeycombs possess high stiffness and strength in out-of-plane directions, and relatively lower mechanical resistance and higher resilience in in-plane directions [3,4]. Therefore, the in-plane configuration of honeycombs is usually utilized in NPTs. In addition, the cell structures of honeycombs are tunable to optimize in-plane properties, e.g. by changing the cell angle, wall thickness, and length to produce tailored stiffness and strength [5–7].

Recently, an attempt has been made to use honeycomb spokes in constructing NPTs in trucks [7]. There are also research works conducted to guide the structural design and optimization of NPTs. For instance, Ju et al. [8] developed finite element models of NPTs with honeycomb structures as a shear band and investigated one-dimensional contact pressure of tires. It was found that the auxetic hexagonal honeycomb shear band designed with a higher negative cell angle provided a lower contact pressure along the contact patch associated with in-plane shear flexible structures. Kim et al. [9] studied the static contact pressure of NPTs with hexagonal-cell honeycomb spokes as a function of vertical loads. They discovered that the contact pressure of NPTs was lower than that of traditional pneumatic tires due to a high lateral spoke stiffness of NPTs. Here, it is worth noting that the load carrying capacity, defined as the displacement of a hub center under a vertical concentrated force, is one of the most important indicators of NPTs. Ju et al. [10] compared two types of NPTs with conventional and auxetic hexagonal honeycombs, and showed that, under the same load carrying capability, conventional hexagonal honeycombs with a highly

* Corresponding author.
E-mail address: fanxueling@mail.xjtu.edu.cn (X. Fan).

https://doi.org/10.1016/j.compstruct.2017.12.044
Received 17 April 2017; Received in revised form 29 October 2017; Accepted 20 December 2017
Available online 21 December 2017
0263-8223/

positive cell angle had low local stresses and mass.

Obviously, most of these works are focused on the static properties and loading response of NPTs. However, NPTs are mainly subjected to dynamic loading in service. Thus, it is necessary to further examine the dynamic performance of NPTs. Other factors such as dynamic material properties and kinetics, have also to be considered in dynamic analyses. Gasmi et al. [11] proposed an analytical model for a compliant NPT rolling on frictionless, rigid ground. Their model was validated by numerical and experimental data. Ma et al. [12] investigated the effects of thickness of a shear band and tread on the performance of NPTs, placing emphasis on impact between NPTs and sand with obstacle. As is well known, rolling resistance is a key parameter to evaluate the performance of a tire. The hysteretic energy loss of a viscoelastic tire material is the main contributor to rolling resistance of the tire, which constitutes 90–95% of the total rolling energy loss [13]. In order to reduce the rolling resistance of a NPT, a shear band made of a porous and fiber-reinforced elastomer was proposed, and numerical simulations were conducted to demonstrate the reduced energy loss by using hyperelastic and viscoelastic material models [14,15]. The influence of geometric and material parameters on overall performance of NPTs has been also analyzed [16–18]. To the best of our knowledge, however, there are few works about the dynamic behaviors of NPTs with honeycomb spokes, especially on their rolling resistance.

In this paper, the static and dynamic behaviors of NPTs with different honeycomb spokes were numerically simulated. Especially, the deformation modes, stress distribution and rolling resistance of NPTs with honeycomb spokes were studied for the first time. The paper is organized as follows. In Section 2, the simulation model is introduced, including the geometric size, material properties and numerical methods. Section 3 contributes to the studies on static properties (deformation modes, stress distribution and load carrying capacity) of NPTs designed with the same cell wall thickness of honeycomb spokes or reference load carrying capacity. Then, in Section 4, the deformation modes, stress distribution and the rolling resistance are discussed under dynamic loading. Finally, conclusions are summarized in Section 5.

2. Simulation model

2.1. Geometric parameters

Three-dimensional finite element models of NPTs were constructed by using the commercial software ABAQUS/Standard. As shown in Fig. 1, NPTs consist of a hub, a number of honeycomb spokes, two rings, a shear band, and a tread. The diameter and cross-sectional width of a NPT were designed to be 664 and 215 mm (according to the National Standards, GBT 2977-2008). The thicknesses of hub, shear band, rings (inner and outer ones) and thread are 1, 9, 0.5 and 5 mm, and the inner radii of hub, shear band and tread are 216, 317.5 and 327 mm, respectively.

As spokes with auxetic hexagonal honeycombs have a much higher mass than that with conventional hexagonal honeycombs, and the properties of auxetic hexagonal honeycombs are more complex than that of hexagonal honeycombs. Thus, only properties of spokes with conventional hexagonal honeycombs were investigated in this paper. The in-plane effective moduli of honeycombs used in a spoke structure were determined in accordance with the theory of cellular materials [19–24], which are given as

$$E_r^* = E_s\left(\frac{a}{l}\right)^3 \frac{\cos\theta}{(h/l + \sin\theta)\sin^2\theta} \tag{1}$$

$$E_\Omega^* = E_s\left(\frac{a}{l}\right)^3 \frac{(h/l + \sin\theta)}{\cos^2\theta} \tag{2}$$

$$G_{r\Omega}^* = E_s\left(\frac{a}{l}\right)^3 \frac{(h/l + \sin\theta)}{(h/l)^2(1 + 2h/l)\cos\theta} \tag{3}$$

where E_r^*, E_Ω^* and G_Ω^* are the effective moduli in radial, circumferential and shear directions, h, l and θ are the average values of the vertical cell length, inclined cell length and cell expanding angle, respectively, as schematically illustrated in Fig. 2, E_s is Young's modulus of a base material, and a is the cell wall thickness. The density of honeycomb can be obtained by

$$\rho^* = \rho_s \frac{a/l(h/l + 2)}{2\cos\theta(h/l + \sin\theta)} \tag{4}$$

where ρ_s is the density of a base material.

As key components of a NPT, the ratio of the inclined cell length to height in honeycomb spokes is a critical parameter to design in-plane flexible structures under tension-compression loading [10]. It can be quantitatively reflected by the cell expanding angle of honeycombs. In this paper, three honeycomb spokes were designed with different cell expanding angles of 15.76°, 31.50° and 47.14°. Three NPTs with a 2 mm cell wall thickness of honeycomb spokes are denoted as NPT–A1, NPT–B1 and NPT–C1, and NPTs with cell expanding angles of 15.76°, 31.50° and 47.14° and different cell wall thicknesses are indicated as NPT–A2, NPT–B2 and NPT–C2, respectively. The geometrical parameters and effective mechanical properties of honeycomb spokes in different types of NPTs are listed in Table 1, and their corresponding models (i.e., NPT–A1, NPT–B1, NPT–C1) are illustrated in Fig. 3.

2.2. Material properties

The hub is assumed to be aluminum alloy (Al 7075–T6) in simulations, and the rings, with a similar shape of airless tires, are a high strength steel (ANSI 4340). The mechanical properties of Al 7075–T6 and ANSI 4340 are given in Table 2.

Polyurethane was used to construct honeycomb spokes and the shear band, while synthetic rubber was for the tread. Both of these two hyperelastic materials were modeled using the Ogden theory [14,23], in which the strain energy function can be represented as

Fig. 1. Photograph of a NPT and illustration of its components with honeycomb spokes.

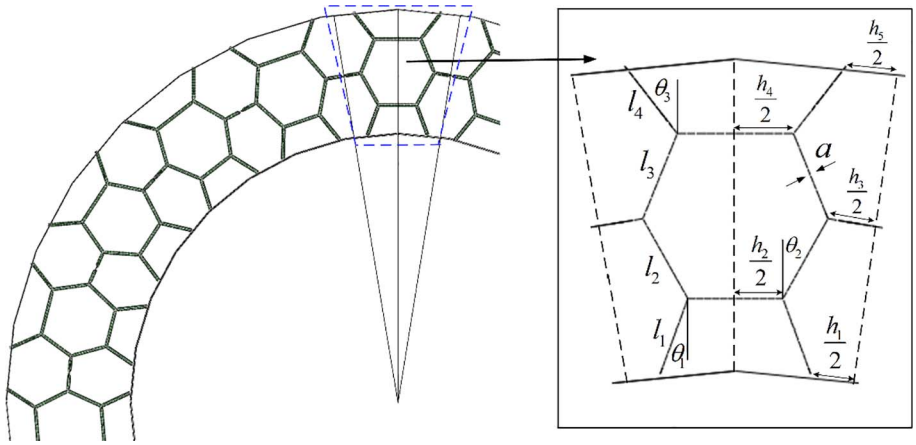

Fig. 2. Schematic illustration of the basic cells of honeycomb spokes and their geometric parameters.

$$W(\lambda_1,\lambda_2,\lambda_3) = \sum_{i=1}^{N} \frac{\mu_i}{\alpha_i}(\lambda_1^{\alpha_i} + \lambda_2^{\alpha_i} + \lambda_3^{\alpha_i} - 3) \tag{5}$$

where W is the strain energy function, λ_i is the deviatoric principal stretch, N is a material parameter, μ_i and α_i are temperature-dependent material parameters (see Table 3).

To quantitatively evaluate the rolling energy loss of a NPT, the viscoelastic properties of polyurethane and synthetic rubber were also considered. The generalized Maxwell model of viscoelastic behavior was implemented with the Prony series by using shear relaxation [14,25], which is given by

$$G_R(t) = G_0\left[1 - \sum_{k=1}^{N} g_i(1 - e^{-t/\tau_i})\right] \tag{6}$$

where $G_R(t)$ is the shear relaxation modulus, G_0 is the instantaneous shear modulus, and g_i and τ_i are Prony relaxation time constants that were used to fit experimental data. The viscoelastic Prony series coefficients in an ascending order of three terms ($N = 3$) for polyurethane and rubber are listed in Table 3. The rolling resistance of NPTs was calculated from the total viscoelastic energy loss (ALLCD in ABAQUS) per unit rolling distance [17,18]. The rolling resistance is expressed as

$$F_R = \frac{W_d}{D} \tag{7}$$

where W_d is the energy dissipated, and D is the distance rolled by a tire.

2.3. Numerical methods

A rigid kinematic coupling constraint is defined so that the outer surface of a hub is coupled to a reference node at the hub center. A vertical load was added at the hub center, and then, an angular velocity of 0.01 rad/ms was applied when investigating the rolling resistance of NPTs. The rigid hub, spokes, inner and outer reinforcements, shear band, and tread were assembled together with a tie constraint. A surface to surface contact interaction was assigned between the road and outer edge of tread. Within the contact zone, friction was implemented in the tangential direction and hard contact was assigned in the normal direction. The friction coefficient was adopted as 0.15, which is a typical value to avoid slip during rolling simulations. Shell elements of type S4R were used for the spoke, hub, and rings, while continuum elements of type C3D8RH were applied for the tread and shear band. The hub and rings were meshed with 20 elements across the tire width and 200 elements around circumference. The honeycomb spokes were meshed with 40 elements along the tire width and 24 elements along the cell length. The shear band and tread were meshed with 40 elements across the tire width, 3 elements along thickness and 400 elements around circumference. The same meshing method was used for different types of NPTs, and the total number of elements in each NPT was 217,440. Based on the studies on mesh sensitivity, it was revealed that the mesh density was sufficient to ensure the numerical accuracy.

3. Static behavior

In simulations, NPTs were designed based on two suggested concepts on honeycomb spokes. One is related to spokes with the same cell wall thickness and the other refers to spokes with the same reference load carrying capability. The static behavior of three types of NPTs were comprehensively investigated.

3.1. NPTs with same cell-wall thickness

3.1.1. Stress distribution

The NPT honeycomb spokes were designed with a constant thickness of 2 mm. In simulations, a concentrated force ranging from 0 to 4 kN was applied at the center of the hub. Here, it is of interest to note that, in the design of NPTs, the stress distributions in spokes and tread are usually concerned. Fig. 4 shows the deformation modes of three types of NPTs when a vertical force of 2.0 kN was applied at the center of the hub. It is seen that only the honeycomb spokes undergo significant deformation. The top half of spokes mainly suffer tension loading, while their bottom half lies in compression and bending. The largest deformation of spokes occurs at the edges in contact with road surface. The displacements of the hub center of NPT–A1, NPT–B1 and NPT–C1 are 10.0, 11.1, and 15.4 mm, respectively. Thus, NPT–C1 honeycomb spokes are obviously most deformed, while NPT–A1 are least deformed. It is believed that the lower cell expanding angle results

Table 1
The geometrical parameters and effective mechanical properties of honeycomb spokes.

Type	l (mm)	h (mm)	θ (°)	a (mm)	ρ^*/ρ_s	E_r/E_s	E_θ/E_s	$E_{r\Omega}/E_s$
NPT–A1(A2)	26.25	36.66	15.76	2.0	0.08	3.46×10^{-3}	8.32×10^{-4}	1.02×10^{-4}
NPT–B1	29.65	28.52	31.50	2.0	0.08	6.40×10^{-4}	7.04×10^{-4}	1.98×10^{-4}
NPT–C1	37.21	16.74	47.14	2.0	0.08	1.92×10^{-4}	5.76×10^{-4}	7.04×10^{-4}
NPT–B2	29.65	28.52	31.50	2.3	0.09	9.73×10^{-4}	1.07×10^{-3}	3.02×10^{-4}
NPT–C2	37.21	16.74	47.14	3.1	0.12	7.15×10^{-3}	2.14×10^{-3}	2.62×10^{-3}

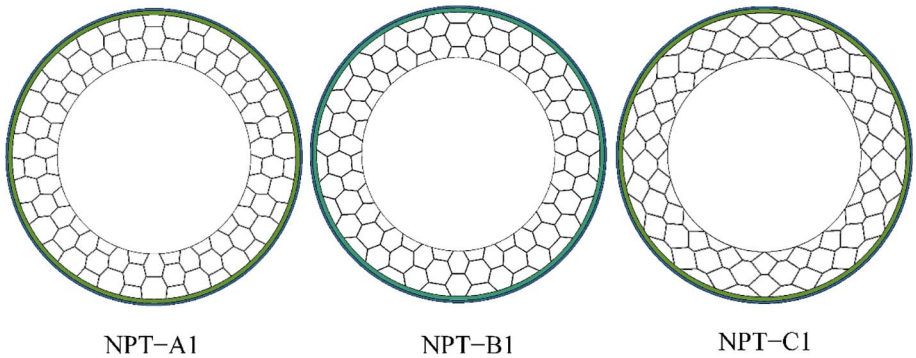

Fig. 3. NPTs designed with a constant cell wall thickness but different cell geometries of honeycomb spokes.

in a higher effective modulus in the radial direction.

The local stress contours of three types of NPTs under a 2 kN vertical force are shown in Fig. 4. The honeycomb spokes were subjected to bending at the contact edges, while the primary compression loading dominated in the radial direction. Elastic bulking can be clearly observed in deformed NPTs. Stress concentration appears at the joint locations of cellular wall edges, and the maximum stresses in three spokes are about 2.088, 1.866 and 2.124 MPa, respectively. As shown in Fig. 5, it is obvious that stresses in different spokes increase evidently with increasing the vertical concentrated force. The maximum stress in spikes of NPT–C1 is the highest, while stresses in NPT–A1 and NPT–B1 are similar. Taking the load carrying capacity into account, the type A1 honeycomb structure used as spokes of NPTs is advantageous over the other two types.

In addition, the maximum contact pressure between the tread and road surface is also considered. As seen in Fig. 6, a rectangular contact shape on the outside surface of tread is developed, and the contact region increases gradually with the increase of vertical force. Contact pressure between the tread of NPT–A1 and outer ring are shown in Fig. 7. Further studies show that the contact pressure between the tread and outer ring is much higher than that between the tread and road surface. Thus, the maximum stress in tread occurs on the spot of internal surface contacted with outer ring. It was also found that the contact pressure is more uniform along the lateral direction than that in the circumferential direction. The evolution of maximum stress in the tread of NPTs under different vertical forces is shown in Fig. 8. It is clearly seen that the three types of NPTs under different vertical forces have almost the same maximum stress in tread. When the vertical concentrated force changes from 1 to 2 kN, deformation in honeycomb structures suddenly rises to a higher level, which may lead to a significant increase of contact pressure of the tread. When the vertical concentrated force is higher than 2 kN, the maximum stress increases slowly with increasing the vertical force. The maximum stress in tread of NPT–A1 is slightly higher than that of NPT–B1 and NPT–C1. However, the maximum contact stress in the tread of NPTs is much lower than that in pneumatic tires, as listed in Table 4. It implies that NPTs can be applied in automobiles.

3.1.2. Load carrying capacity

Load carrying capacity is one of the most important factors in the design of NPTs, which can be characterized by the displacement of a hub center. The load carrying capacity of NPTs (i.e., force-displacement curves at the center of hub) were compared with that of pneumatic tires (see Fig. 9). It is evident that the displacement of the hub center of NPT–A1 is lowest, while NPT–C1 is highest due to the fact that effective moduli in the radial of honeycomb spokes of TNPT–A1 is highest while that of NPT–C1 is lowest. The results indicate that NPT–A1 has the highest load carrying capacity while NPT–C1 has the lowest when the cell wall thickness is the same. In addition, the load carrying capacities of NPT–A1 and NPT–B1 are close to that of pneumatic tires when the concentrated force is less than 4 kN. When the concentrated force reaches to 4 kN, the load carrying ability of NPT–B1 and NPT–C1 decreases obviously, while NPT–A1 performs well as the load carrying capacity is close to that of pneumatic tires.

Table 3
Coefficients of the Ogden hyperelastic strain energy function and viscoelastic Prony series for polyurethane and synthetic rubber [14].

	Polyurethane				Synthetic rubber			
i	μ_i (MPa)	α_i	g_i	τ_i	μ_i (MPa)	α_i	g_i	τ_i
1	13.546	1.513	0.125	0.002	13.356	1.633	0.200	0.002
2	−2.338	2.212	0.125	0.020	−6.631	1.900	0.200	0.020
3	0.093	−2.471	0.125	0.200	0.058	−2.456	0.200	0.200

3.2. NPTs with same reference load carrying capacity

3.2.1. Load carrying capacity

As mentioned above, NPT–A1 has the highest load carrying capacity when the cell wall thickness of honeycombs is the same, and the displacement of the hub center is 10.0 mm under a 2 kN concentrated force. Next, three types of NPTs were designed to achieve the reference load carrying capacity of a vertical displacement of 10.0 mm of the hub center under a 2 kN concentrated force, through changing the thickness of honeycomb spokes. Consequently, the cell wall thickness of NPT–A2, NPT–B2 and NPT–C2 is 2.0, 2.3 and 3.1 mm, respectively. The dimensions and effective mechanical properties of honeycomb spokes are given in Table 1.

The corresponding load carrying capacity of three NPTs were compared with that of pneumatic tires, as shown in Fig. 10. It is obvious that the displacement of the hub center of NPT–C2 is lowest when the concentrated force is lower than the reference load of 2 kN, implying that NPT–C2 has the highest load carrying capacity. However, the load carrying capacity of NPT–C2 is lowest when the concentrated force is higher than the reference load. In addition, the load carrying capacities of NPT–A2 and NPT–B2 are almost the same under different applied forces.

Table 2
Material properties of hub (7075–T6) and inner/outer rings (ANSI 4340) [14].

Material	Density (kg/m^3)	Young's modulus (GPa)	Shear modulus (GPa)	Poisson's Ratio	Yield strength (MPa)	Yield strain (%)
Aluminum-alloy (7075-T6)	2800	72	27	0.33	503	0.71
High strength steel (ANSI 4340)	7800	210	76	0.29	1240	0.59

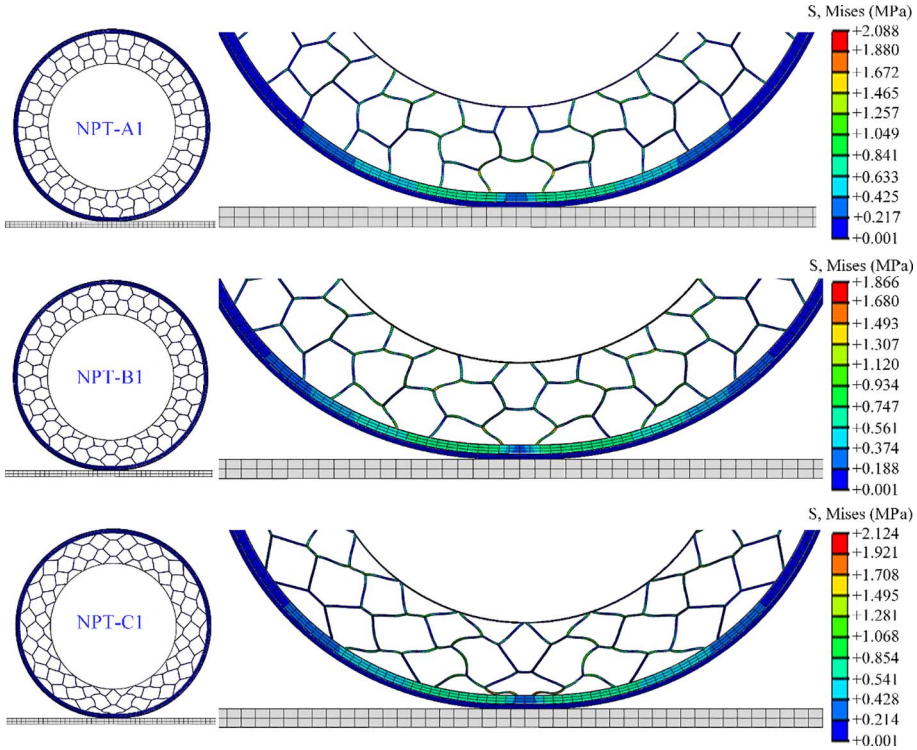

Fig. 4. Deformation modes and local stress contours of NPTs under a vertical force of 2 kN.

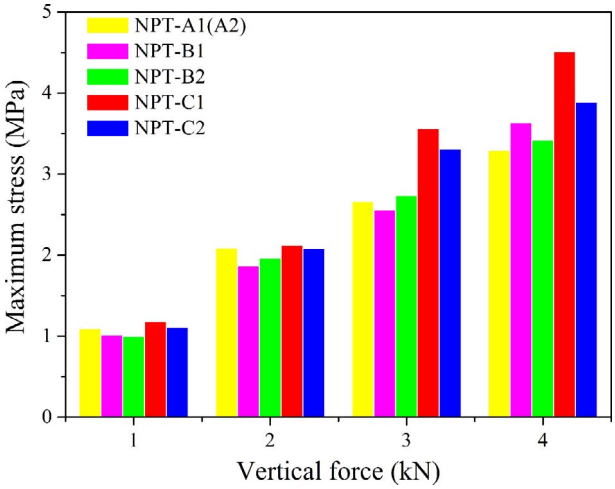

Fig. 5. Maximum stresses in the spokes of NPTs subjected to different vertical forces.

The mass of NPTs is another important parameter that should be minimized to reduce energy consumption. The difference in the masses of three types of NPTs is solely due to different masses of honeycomb spokes, as shown in Table 4. In the condition of same load carrying capacity, masses of the honeycomb spokes of NPT–A2, NPT–B2 and NPT–C2 are 3098, 3632 and 5371 g, respectively.

With consideration of all these factors, it is suggested that honeycomb spokes in NPT–A2 have more advantages than others in applications.

3.2.2. Stress distribution

The maximum stress in spokes and tread of NPTs with different thicknesses of spokes are shown in Fig. 5 and Fig. 8, respectively. The distributions of maximum stress in spokes and tread are similar to those of three types of NPTs with the same cell wall thickness. In addition, when NPTs were designed with same reference load carrying capacity, the difference of maximum stress in treads is smaller than that of NPTs designed with the same cell wall thickness. It should be pointed out that, however, the mass of NPT–A2 is the lowest in both cases, as seen in Table 4. Since mass of NPTs may significantly influence energy dissipation, NPT–A2 seems to be the best, which is further discussed in the dynamic behavior of NPTs.

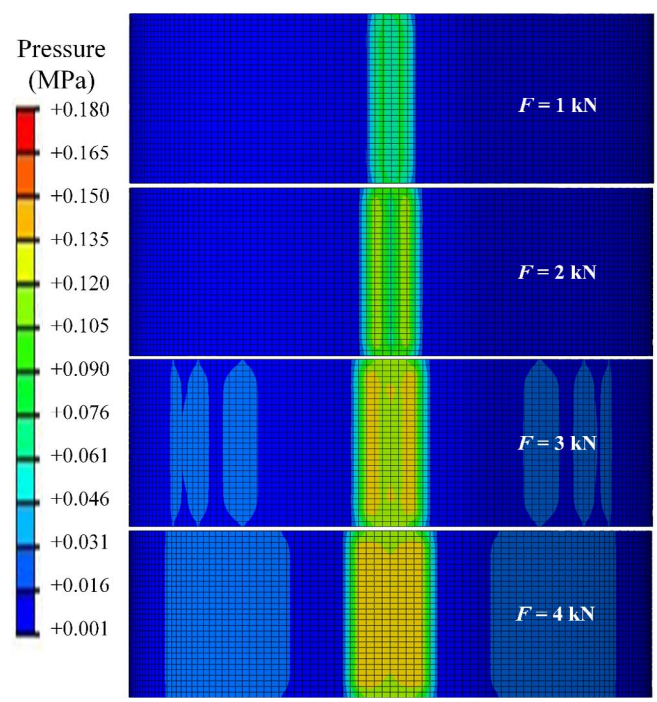

Fig. 6. Evolution of the contact pressure between the tread of NPT–A1 and road surface with the increase of vertical force.

4. Dynamic behavior

In consideration of a relatively low stress in NPTs, only the dynamic

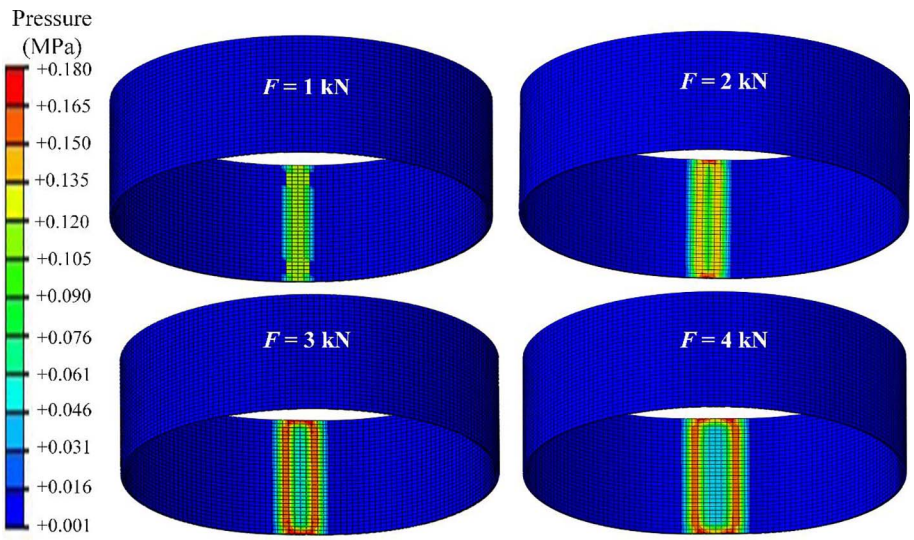

Fig. 7. Evolution of the contact pressure between the tread of NPT–A1 and outer ring with the increase of vertical force.

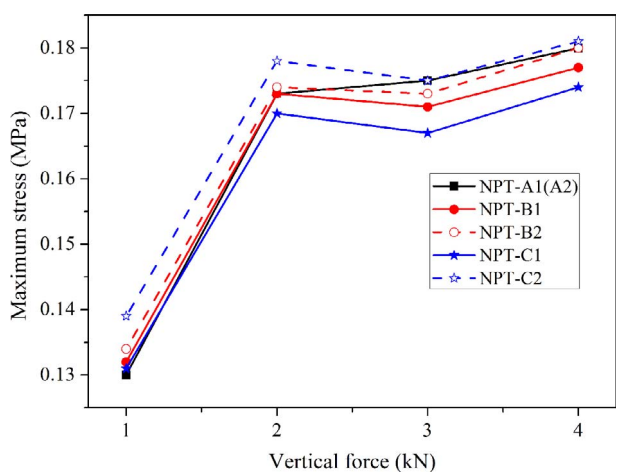

Fig. 8. The maximum stress in the tread of NPTs under different vertical forces.

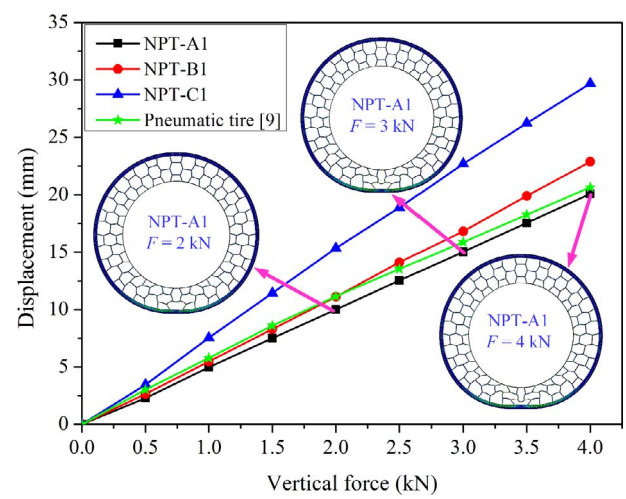

Fig. 9. The load carrying capacities of three NPTs designed with the same cell-wall thickness compared with that of a pneumatic tire [9].

behavior of NPTs designed with same reference load carrying capacity are discussed here.

4.1. Deformation modes

An angular velocity of 0.01 rad/ms (i.e., 3.32 m/s with a radius of 332 mm) was applied at the hub center to simulate the dynamic behavior of NPTs. In simulations, the angular velocity of hub center gradually increased and then reached a steady value at 200 ms. The deformation modes of NPT–A2 under a vertical force of 4 kN together with experimental observations are shown in Fig. 11 [26]. Compared with deformation of spokes under static loading (see Fig. 4), dynamic deformation is much larger. The honeycomb spokes mainly experience cyclic tension-compression loading. The largest tensile deformation occurs on the top of spokes, while the largest compression and bending deformation appears on the lower part of spokes. The honeycomb

Table 4
The load carrying capacity and the maximum stress in spokes and treads of NPTs.

Displacement/maximum stress	Vertical force	NPT–A1(A2)	NPT–B1	NPT–B2	NPT–C1	NPT–C2	PT [9]
Displacement (mm)	1 kN	4.920	5.48	4.72	7.54	4.20	5.78
Spoke (MPa)		1.094	1.013	0.998	1.177	1.107	
Tread (MPa)		0.13	0.132	0.134	0.131	0.139	
Displacement (mm)	2 kN	10.01	11.11	9.80	15.35	9.82	11.15
Spoke (MPa)		2.088	1.866	1.960	2.124	2.081	
Tread (MPa)		0.173	0.173	0.174	0.170	0.178	
Displacement (mm)	3 kN	15.06	16.81	15.00	22.70	16.00	15.88
Spoke (MPa)		2.662	2.556	2.738	3.562	3.310	
Tread (MPa)		0.175	0.171	0.173	0.167	0.175	0.43
Displacement (mm)	4 kN	20.09	22.88	20.30	29.69	22.10	20.66
Spoke (MPa)		3.295	3.634	3.419	4.507	3.888	
Tread (MPa)		0.180	0.177	0.180	0.174	0.181	

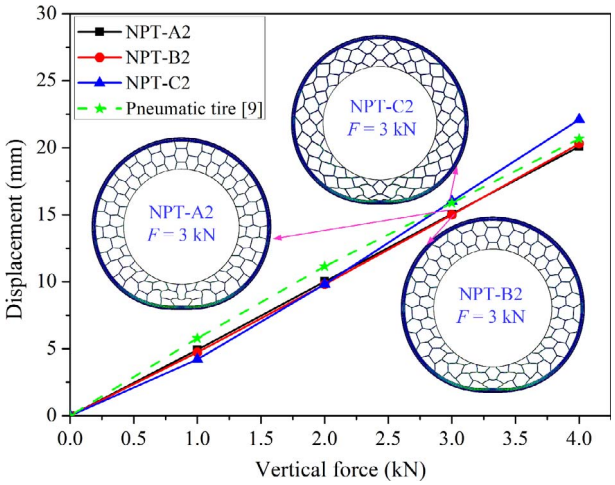

Fig. 10. The load carrying capacities of three NPTs designed with the same reference load carrying capacity compared with that of a pneumatic tire [9].

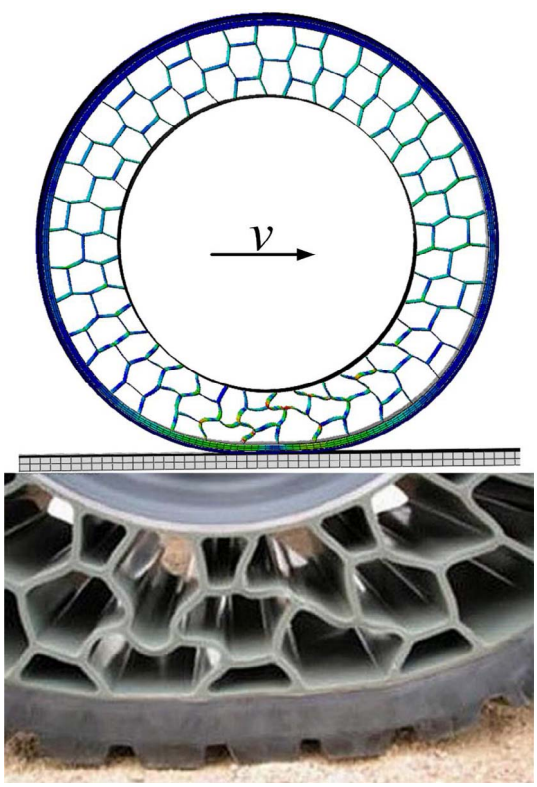

Fig. 11. Comparison of the deformation modes between simulation and experimental results [26].

spokes are subjected to bending at the contact edges as well as the primary compression loading in the radial direction. Elastic buckling is also observed in spokes. It is clear that deformation modes in simulations are in consistent with ones observed in experiments. That is, it is confirmed that the simulation results are reliable.

4.2. Stress distribution

The maximum stresses in spokes vary with rolling of NPTs. The maximum stresses in spokes of NPT–A2 are shown in Fig. 12 under a vertical concentrated force of 2 kN and a rotational force, as well as their comparison with that of NPT–A2 under a static vertical load. It is clearly seen that the maximum stress in spokes increases with the increase of angular velocity. When the angular velocity reaches 0.01 rad/

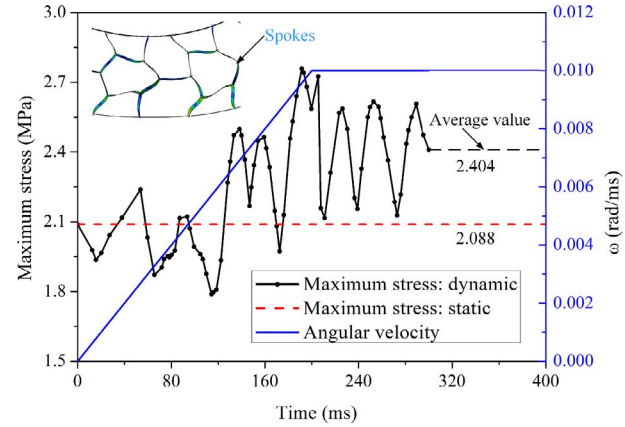

Fig. 12. Comparison of the maximum stress in spokes of NPT–A2 under static and dynamic loads.

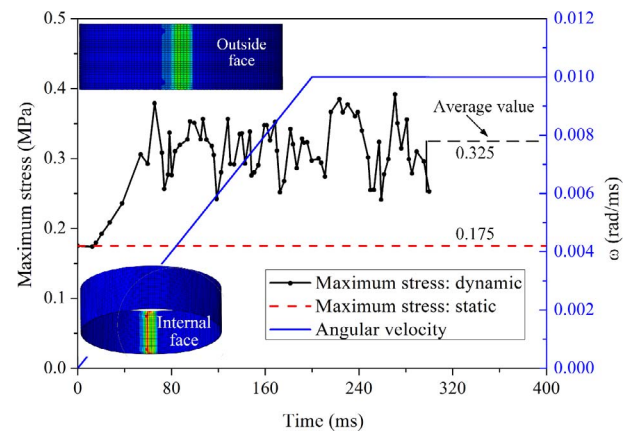

Fig. 13. Comparison of the maximum stress in the tread of NPT–A2 under static and dynamic loads.

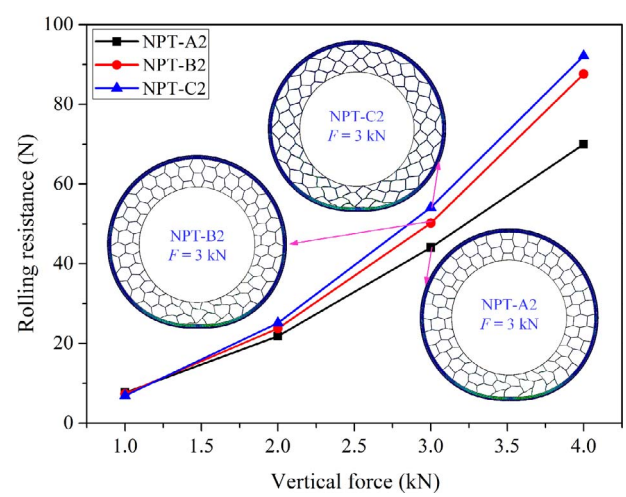

Fig. 14. Rolling resistance of NPTs under different vertical forces.

ms, the maximum stress attains a maximum value. Then, the maximum stress changes periodically with an average value of 2.404 MPa, which was about 15% higher than 2.088 MPa under a static load of 2 kN.

Similar to that of spokes, stresses in the tread also vary when a NPT is rolling. To highlight the difference of maximum stresses in the tread under static and dynamic loads, a comparative study was made for NPT–A2 under a vertical concentrated force of 2 kN. As shown in Fig. 13, the stress in tread reaches the maximum much faster than that

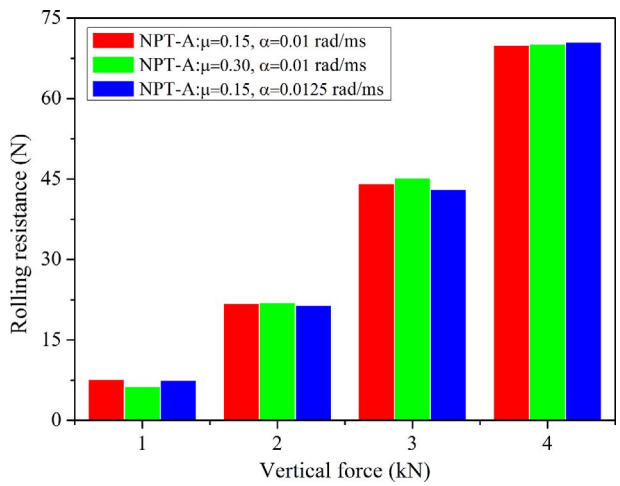

Fig. 15. Comparison of the rolling resistance obtained with different friction coefficients and angular velocities for NPTs.

in spokes, and then begins to wave periodically with an average value of 0.325 MPa. Compared with the maximum stress of 0.175 MPa under a static load of 2 kN, the maximum stress under dynamic loading increases by 85.7%.

4.3. Rolling resistance

The rolling resistance of NPTs is defined as the total viscoelastic energy loss (ALLCD in ABAQUS) per unit rolling distance (see Section 2.2), which was calculated when NPTs rolled at a steady and maximum speed. The rolling resistance of NPT–A2, NPT–B2 and NPT–C2 under different vertical forces at an angular speed of 0.01 rad/ms is shown in Fig. 14. It is seen that the rolling resistance of three NPTs is almost the same when the vertical force is below 1 kN, but it increases significantly with the increase of the vertical force. NPT–A2 and NPT–C2 have the highest and lowest rolling resistance, respectively. This is mainly caused by the lowest mass and smallest deformation of honeycomb spokes of NPT–A2.

The effects of friction coefficient and angular velocity on the rolling resistance of NPTs were also studied. The friction coefficient and angular velocity were chosen to be 0.15 and 0.01 rad/ms in simulations as discussed above. Other two cases were considered with friction coefficient and angular velocity being 0.30 and 0.01 rad/ms, 0.15 and 0.0125 rad/ms, respectively. The results of rolling resistance are shown in Fig. 15. There is no evident difference in rolling resistance obtained with different friction coefficients and angular velocities. Thus, it is concluded that the influence of friction coefficient and angular velocity on rolling resistance of NPTs can be neglected.

The foregoing analyses indicate that both spokes and tread are under a relatively low stress state under either static or dynamic loading. Therefore, the design of NPTs should be mainly based on the load carrying capacity and rolling resistance. Taking all these factors into account, NPT–A2 with a cell expanding angle of 15.76° performs the best. Thus, it is suggested that NPT–A2 is an optimal design in real applications.

5. Conclusions

The static and dynamic behaviors of non-pneumatic tires (NPTs) with honeycomb spokes were investigated by numerical simulations. The focus is mainly on the stress distribution and rolling resistance of NPTs. Three NPTs with different geometric parameters but same cell wall thickness or load carrying capacity were considered. The conclusions can be summarized as follows:

(1) For three NPTs designed with the same cell wall thickness of honeycomb spokes, the maximum stress in spokes of NPT–C1 with a higher cell expanding angle is the highest, but the load carrying capacity of NPT–A1 with a lower cell expanding angle is the highest.
(2) For three NPTs designed with the same reference load carrying capacity, the mass of spokes of NPT–A2 with a lower cell expanding angle is the lowest, while the load carrying capacity is the highest. The maximum stresses in spokes and tread under dynamic loading are much higher than that under static loading.
(3) The rolling resistance of NPT–A2 with a lower cell expanding angle is the lowest under the same vertical concentrated force, due to the lowest mass and smallest deformation of honeycomb spokes. In addition, the friction coefficient and angular velocity have negligible effect on the rolling resistance of NPTs
(4) Taking all the relevant factors into account, the design of NPT–A1(A2) with a cell wall thickness of 2 mm and a cell expanding angle of 15.76° is optimal.

Acknowledgments

This work was supported by the National Natural Science Foundation of China (Grant No. 11472204) and the Fundamental Research Funds for the Central Universities. C. Lu is grateful to the support from the Open Fund of State Key Laboratory for GeoMechanics and Deep Underground Engineering, China University of Mining & Technology (Beijing) (SKLGDUEK1516).

References

[1] Cho JR, Kim KW, Yoo WS, Hong SI. Mesh generation considering detailed tread blocks for reliable 3D tire analysis. Adv Eng Softw 2004;35:105–13.
[2] Rhyne T, Cron SM. Development of a non-pneumatic wheel. Tire Sci Technol 2006;34:150–69.
[3] Gibson LJ, Ashby MF. Cellular solids: structure and properties. Cambridge: Cambridge University Press; 1999.
[4] Lu GX, Yu TY. Energy absorption of structures and materials. Cambridge: Woodhead Publishing Ltd; 2003.
[5] Sun YT, Wang B, Pugno N, Wang B, Ding Q. In-plane stiffness of the anisotropic multifunctional hierarchical honeycombs. Compos Struct 2015;131:616–24.
[6] Li YM, Abbès F, Hoang MP, Abbès B, Guo YQ. Analytical homogenization for in-plane shear, torsion and transverse shear of honeycomb core with skin and thickness effects. Compos Struct 2016;140:453–62.
[7] Zhang QC, Yang XH, Li P, Huang GY, Feng SS, Shen C, et al. Bioinspired engineering of honeycomb structure – Using nature to inspire human innovation. Prog Mater Sci 2015;74:332–400.
[8] Ju J, Ananthasayanam B, Summers JD, Joseph P. Design of cellular shear bands of a non-pneumatic tire-investigation of contact pressure. SAE Int J Pass Cars 2010;3:598–606.
[9] Kim K, Ju J, Kim D. Static contact behaviors of a non-pneumatic tire with hexagonal lattice spokes. SAE Int J Passeng Cars – Mech Syst 2013;6(3):1518–27.
[10] Ju J, Kim DM, Kim K. Flexible cellular solid spokes of a non-pneumatic tire. Compos Struct 2012;94:2285–95.
[11] Gasmi A, Joseph PF, Rhyne TB, Cron SM. Development of a two-dimensional model of a compliant non-pneumatic tire. Int J Solids Struct 2012;49:1723–40.
[12] Ma JF, Summers JD, Joseph PF. Numerical investigation of effect of membrane thickness on the performance of cellular shear band based non-pneumatic tire. In: Proceedings of the ASME 2011 international design engineering technical conferences & computers and information in engineering conference, Washington, DC, USA; 2011.
[13] Walter J, Conant F. Energy losses in tires. Tire Sci Technol 1974;2(4):235–60.
[14] Ju J, Veeramurthy M, Summers JD, Thompson L. Rolling resistance of a non-pneumatic tire having a porous elastomer composite shear band. Tire Sci Technol 2013;41(3):154–73.
[15] Kim K, Heo H, Uddin M, Ju J, Kim DM. Optimization of non-pneumatic tire with hexagonal lattice spokes for reducing rolling resistance, SAE Technical Paper 2015; 01–1515.
[16] Ju JY, Summers JD. Compliant hexagonal periodic lattice structures having both high shear strength and high shear strain. Mater Des 2011;32:512–24.
[17] Jang IG, Sung YH, Yoo EJ, Kwak BM. Pattern design of a non-pneumatic tyre for stiffness using topology optimization. Eng Optimiz 2012;44:119–31.
[18] Veeramurthy M, Ju J, Thompson LL, Summers JD. Optimization of geometry and material properties of a non-pneumatic tyre for reducing rolling resistance. Int J Vehicle Des 2014;66(2):193–216.
[19] Balawi S, Abot JL. The effect of honeycomb relative density on its effective in-plane elastic moduli: an experimental study. Compos Struct 2008;84:293–9.

[20] Heo H, Ju J, Kim DM. Compliant cellular structures: application to a passive morphing airfoil. Compos Struct 2013;106:560–9.
[21] Jin T, Zhou ZW, Wang ZH, Wu GY, Shu XF. Experimental study on the effects of specimen in-plane size on the mechanical behavior of aluminum hexagonal honeycombs. Mater Sci Eng, A 2015;635:23–35.
[22] Sun YL, Li QM. Effect of entrapped gas on the dynamic compressive behavior of cellular solids. Int J Solids Struct 2015;63:50–67.
[23] Qwamizadeh M, Lin M, Zhang Z, Zhou K, Zhang YW. Bounds for the dynamic modulus of unidirectional composites with bioinspired staggered distributions of platelets. Compos Struct 2017;167:152–65.
[24] Fu MH, Chen Y, Hu LL. A novel auxetic honeycomb with enhanced in-plane stiffness and buckling strength. Compos Struct 2017;160:574–85.
[25] Abaqus Version 6.14. Abaqus analysis user's guide. Dassault Systèmes Simulia Corp. Providence, USA; 2014.
[26] http://my.tv.sohu.com/us/133251931/ 52639794.shtml.